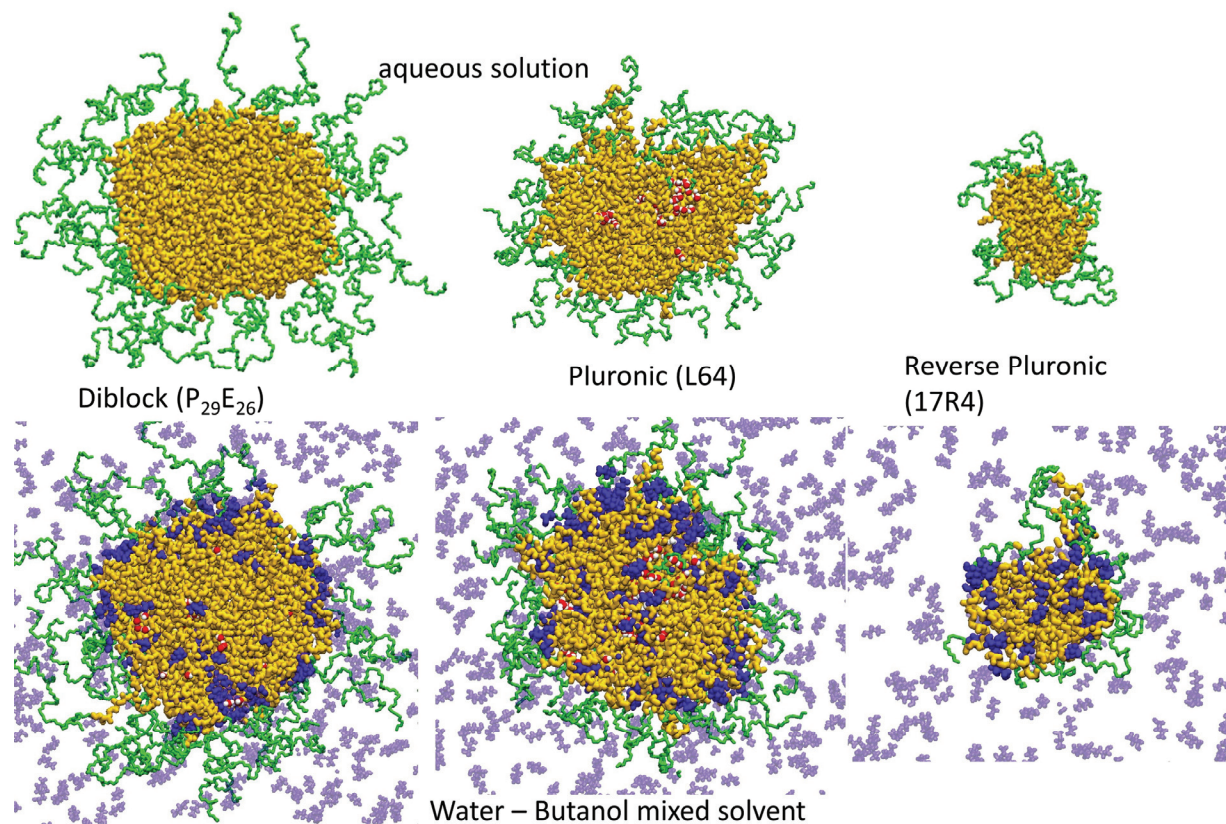


Molecular structure and co-solvent distribution in PPO-PEO and Pluronic micelles

Rasika Dahanayake and Elena E. Dormidontova*

Polymer Program, Institute of Materials Science and Department of Physics, University of Connecticut, Storrs, CT, 06269

For Table of Contents use only:



Abstract

The structure and properties of micelles formed by diblock and triblock copolymers containing polypropylene oxide (PPO) and polyethylene oxide (PEO) in aqueous solutions are affected by chain architecture and have important implications for applications, e.g. in the biomedical area. Using atomistic molecular dynamics simulations we investigate and compare the molecular structure of diblock copolymer $\text{PPO}_{29}\text{PEO}_{26}$, Pluronic L64 and reverse Pluronic 17R4 micelles formed by block copolymers of the same length and composition, but different distribution of PPO and PEO blocks, in pure aqueous solution or with 5% (by volume) added co-solvents. We show that while the diblock copolymer forms a tightly packed mostly spherical micelle, Pluronic L64 micelles are non-spherical, contain 10-18% (by volume) of water in the loosely packed PPO core partially interpenetrated by the PEO block. Reverse Pluronic 17R4 micelles are rather small, but relatively well-packed. Addition of 5% (by volume) of alcohol to aqueous micelle solutions results in a minimal change in the case of ethanol, while addition of butanol or hexanol leads to an increase of water content in the core and alcohol accumulation at the core-corona interface for the $\text{PPO}_{29}\text{PEO}_{26}$ micelle. For L64 micelles alcohol makes micelles more spherical, but enhances defects, e.g. concentrates water in the core center or enhances PEO penetration, depending on the aggregation number. For 17R4 micelles butanol and especially hexanol penetrate into micelle core, swelling it. Even stronger core swelling occurs upon addition of 5% (by volume) of isobutyric acid to aqueous solution of $\text{PPO}_{29}\text{PEO}_{26}$ micelles. We show that the extent of co-solvent penetration and its distribution within the micelles strongly depend on co-solvent hydrophobicity, capability of hydrogen bond formation with polymer and micelle architecture can affect micelle properties and performance in practical applications.

Introduction

Water-soluble responsive polymers and their self-assembled structures are actively used in many (nano)technological applications including biomedicine.^{1–5} Polyethylene oxide (PEO) and polypropylene oxide (PPO) and their self-assembled diblock and triblock copolymer Pluronic micelles are among the most commonly used polymeric materials in biomedical applications.^{5,6} While these micelles have been extensively investigated experimentally, theoretically and by computer simulations,^{7–12} some conformational and structural details of the self-assembled structures remain unknown or under debate, e.g. the presence of water in the core or block interpenetration within the micelles, especially in the presence of co-solvents. One of the reasons for this uncertainty is the complex competition between volume interactions and hydrogen bonding with solvent, both of which affect polymer conformation and aggregation and are difficult to assess experimentally or via coarse-grained simulations. Atomistic molecular dynamics simulations can provide such insights, but so far there have been very few studies on the subject.^{7,8} Here we apply atomistic molecular dynamics simulations to investigate and compare structure and properties (including solvent distribution and polymer hydration) of PPO-PEO diblock copolymer and triblock copolymer Pluronic and reverse Pluronic micelles in aqueous solution and upon addition of co-solvents such as isobutyric acid and alcohols of different hydrophobicity.

A large variety of diblock and triblock copolymers containing PPO and PEO blocks have been developed and investigated experimentally and theoretically.^{5,13–16} Overall, it has been shown that micelle formation (critical micelle temperature and critical micelle

concentration), stability and properties depend on the temperature and block lengths.^{14,15,17–20} The solubility of PPO in water decreases with temperature and the polymer becomes insoluble above a certain temperature which depends on its molecular weight.^{21,22} As a result, PPO-containing micelle formation and properties are strongly affected by the temperature and PPO length. There is a general agreement that micelle cores formed by PPO blocks are not as dense as in the case of more hydrophobic polymers and these micelles have a relatively broad interface with interpenetration of PPO and PEO blocks. There seems to be a large variation in estimates of micelle aggregation numbers and core sizes for the same block copolymer, assessment of the presence of water within the core or micelle shape (e.g. spherical vs ellipsoidal).^{19,23–25} Thus, for L64 Pluronic micelle PEO₁₃PPO₃₀PEO₁₃ (further abbreviated as E₁₃P₃₀E₁₃) Alexandridis et al²⁶ arrived at aggregation number 40 at 47°C, Booth et al²⁴ reported an aggregation number 60 at 50°C, Ulbright et al¹⁹ estimated it to be 64 at 46°C, while Chu et al²⁵ came up with an aggregation number of 88 at 42.5°C and 225 at 47.5°C and Hasan et al²³ arrived at an estimate of 170 for the aggregation number at 45°C. These reported differences might be attributed to possible variations in micelle preparation methodology, which is known to affect the aggregation number for kinetically trapped micelles, but the block lengths for L64 are short and weakly hydrophobic making kinetic trapping less of an issue. On the other hand aggregation number estimates strongly depend on the models and assumptions on solvent content of the core used to analyze experimental scattering data.^{26,27} One complexity in understanding the behavior of PPO- and PEO-containing micelles is the reliance of these polymers on hydrogen bonding with water for their solubility. Thus, understanding the distribution of water throughout the

micelles is important for prediction of their properties, stability and success of applications in aqueous media, but it is not easy to assess experimentally.

Furthermore, micelle properties may also be significantly affected by the polymer architecture. Thus, Booth et al ²⁴ compared the properties of micelles formed by diblock P₂₉E₂₆ and triblock L64 (E₁₃P₃₀E₁₃), copolymers of similar molecular weights, but containing either one longer PEO block in the diblock or two shorter PEO blocks in triblock. They found that while aggregation numbers were comparable (67 for diblock and 60 for triblock), diblock copolymer micelles were more tightly packed and have a different area per chain than in the corresponding triblock copolymer micelle. An even stronger difference in the behavior of Pluronic L64 (E₁₃P₃₀E₁₃) micelles and reverse Pluronic 17R4 (P₁₄E₂₄P₁₄) of comparable compositions but different monomer distribution along the chain have been observed. ²⁵ Chu et al ²⁵ demonstrated that while L64 and 17R4 Pluronics both form micelles at 42.5°C and 40°C respectively, L64 has a lower critical micelle concentration and noticeably higher aggregation number (88) compared to 17R4 (aggregation number 10). Reverse Pluronics exhibit a weaker aggregation capability, not only because of the longer PEO block (and therefore better solubility), but primarily because of the shorter PPO block, for which the solubility is highly sensitive to temperature.^{21,22,28} As these examples demonstrate, for these polymers not only is the total hydrophobic/hydrophilic balance important, but also the specific distribution of PEO and PPO monomers along the chain which in turn influences block packing in the micelle and solvent distribution. Computer simulations can provide significant insights into these properties.

Another line of research that has been explored experimentally is the effect of co-solvents on the micellization and properties of Pluronics. Several experimental groups investigated the effect of alcohols of different hydrophobicity (alkane lengths) on the micellization of Pluronics.^{29–33} It has been found that short alcohols, such as ethanol, increase the critical micelle temperature (CMT) and increase polymer solubility while longer, more hydrophobic alcohols such as hexanol have the opposite effect: decrease of CMT and an increase in micelle aggregation number indicating a stronger tendency for micellization.^{29–34} Using NMR (NOESY) for micelles formed by P104 Parekh et al. demonstrated that the hydroxyl group of the alcohol co-localized near the PEO and likely was located at the interface, while the methyl tail of longer alcohols is located in the micelle interior,³² attesting to alcohol penetration into the core leading to its dehydration.³³ Among other solvents formamide and urea are found to decrease the aggregation number and micelle size, while glycerol, glucose or glycine had the opposite effect.^{30,34} The influence of co-solvents on Pluronic micelles can be rather complex, as they can simply change the interfacial tension or preferentially interact with PPO or PEO blocks or compete for hydrogen bonding with water. All of these factors can contribute to the experimentally observed behavior and it is difficult to distinguish which factor plays the dominant role without molecular level resolution, which can be provided by computer simulations.

Micellization of Pluronics has been investigated theoretically^{14,15,18,20,35} and by means of computer simulations.^{7–12,36,37} Predictions have been made regarding the PPO and PEO block density distribution^{7,8,20,35} in Pluronic micelles, micelle capability to encapsulate

hydrocarbons and drugs^{9,14,15,18,37} or interact with lipid bilayers.^{11,12} Due to the large size of the system significant computational resources are required and to date there have been only a few studies that provide atomistic resolution of the micelle structure of Pluronics.⁷⁻⁹ Roccarano *et al.* used an atomistic OPLS forcefield to investigate the interaction of a few P85 Pluronic molecules with curcumin in aqueous solution.⁹ As expected, they found preferable interactions of curcumin with PPO, while the PEO remains well solvated by water. Bedrov *et al*^{7,8} used a coarse grained implicit solvent model to equilibrate L64 and F127 pluronic micelles, which were consecutively backmapped to an atomistic level and further equilibrated to investigate the micelle structure. They obtained the volume fraction distribution throughout the micelle of the PPO and PEO blocks and water and determined that the L64 micelle (with aggregation number 40) has an ellipsoidal shape with a core of 3.4nm in radius (on average) and contains about 8% (by volume) water distributed within the core.⁷ Apart from these studies we are not aware of any computer simulations at the atomistic level which elucidate the structure of PPO/PEO diblock or triblock copolymer micelles in aqueous solution or mixed solvents.

Here using atomistic OPLS-based molecular dynamics simulations we investigate and compare micelle structures, polymer and water distribution in the diblock copolymer P₂₉E₂₆ micelle, triblock copolymer E₁₃P₃₀E₁₃, Pluronic L64, and P₁₄E₂₄P₁₄, reverse Pluronic 17R4, micelles, all formed from block copolymers of nearly the same length, but varying in block distribution. We compare the molecular level details of the micelle structures and analyze the effect of block lengths and monomer distribution (diblock vs

triblock, Pluronic vs reverse Pluronic) on micelle shape and intrinsic structure. In the case of the Pluronic L64 we also consider the impact of the aggregation number. Co-solvent localization and potential changes in micelle structure occurring within the initial 130ns after introduction of 5% (by volume) alcohols of different hydrophobicity (ethanol, butanol, hexanol) are analyzed together with the dynamics of solvent exchange in the micelle core. In the case of a diblock copolymer we also investigate the effect of addition of glycine or isobutyric acid, which are capable of stronger hydrogen bonding with polyethers^{38,39} than simple alcohols. We compare our results with available experimental literature data and make conclusions regarding the micelle sensitivity to the presence of co-solvent for different polymer architectures, that provide important insights regarding the interpretation of experimental data and applications of Pluronic micelles in the biomedical area.

Computational Details

We performed atomistic molecular dynamics simulations of micelles in aqueous solution. The simulations were performed using the GPU-enabled version of GROMACS 2020.4 on the Extreme Science and Engineering Discovery Environment (XSEDE)⁴⁰ cluster using the OPLS force-field⁴¹ with SPC/E water model.^{42,43} The force-fields for PPO and PEO are the same as in our earlier papers on the behavior of corresponding polymers in aqueous solutions.^{28,39} The standard OPLS force fields for isobutyric acid (IBA) and glycine have been used, while for alcohols (ethanol, butanol, hexanol) refined force fields^{44,45} were employed. The polymer micelles were pre-assembled from monodisperse copolymers using packmol^{46,47} and had the following aggregation numbers based on experimentally reported values: 67 for P₂₉E₂₆ and 12 for P₁₄E₂₄P₁₄, reverse Pluronic

17R4, and several aggregation numbers: 40, 50 and 76 for E₁₃P₃₀E₁₃, Pluronic L64.^{8,13,19,24–26,48} The details of micelle simulations and methodology of co-solvent addition is discussed in Supporting Information. The simulations were performed with NPT ensemble with a pressure of 1 bar in periodic boxes ranging from 12 x 12 x 12 nm³ to 20 x 20 x 20 nm³. The simulations were performed at 47 °C, where all micelles are known to be stable. The temperature coupling was done using the v-rescale thermostat with a coupling constant of 1 ps. The bonds were constrained using the LINCS algorithm. Pressure coupling was carried out using the Berendsen barostat for the initial 30 ns of equilibration time. Then the production run was continued with the Parinello-Rahman barostat for 100ns with a coupling constant of 1ps. The integration time step for simulations were 2fs. Electrostatic interactions were calculated using PME (Particle-Mesh Ewald) summation. A long range dispersion correction was applied for energy and pressure.

To characterize the micelle core shape we used anisotropy (κ^2).

$$\kappa^2 = \frac{3}{2} \frac{\lambda_1^4 + \lambda_2^4 + \lambda_3^4}{(\lambda_1^2 + \lambda_2^2 + \lambda_3^2)^2} - \frac{1}{2} \quad (1)$$

Where, λ_1 , λ_2 and λ_3 are the principal moments (eigen values) of the gyration tensor with $\lambda_1 > \lambda_2 > \lambda_3$, where the radius of gyration for the micelle core is $R_g = \sqrt{(\lambda_1^2 + \lambda_2^2 + \lambda_3^2)}$. The anisotropy changes between 0 and 1, where zero indicates a spherically symmetric core and 1 corresponds to an elongated rod-like shape.

The volume fraction profiles of the polymer micelles in aqueous solutions and mixed solvent were calculated with respect to the center of mass of the micelle core using spherical shells of 0.6nm thickness using 2500 frames spanning 20ns of the production

run. The following volumes were considered for the oxygen atoms: 0.016nm³; for the CH₂ group: 0.025nm³, for CH₃ groups: 0.033nm³, for CH and NH groups: 0.02nm³ and for water molecules 0.03nm³.^{49,50} To characterize the interfacial width the number density distribution for the PPO carbon atom closest to the chemical bond between PPO and PEO blocks was calculated with respect to the center of mass of the core over the same number of frames and time as the volume fraction calculations.

To further understand the dynamics of water and co-solvent molecules within the micelle core the following residence time correlation C(t) was calculated:

$$C(t) = \langle \frac{N_s(t)}{N_s(t_0)} \rangle \quad (2)$$

where N_s(t₀) is the number of water or co-solvent molecules in the micelle core at time t₀ = 0 and N_s(t) is the number of the original molecules that remain within the core at time t. The visualization of the simulation results was performed using Visual Molecular Dynamics (VMD).⁵¹

Results and Discussion

First, we analyzed the properties of an equilibrated PEO₂₆PPO₂₉ (P₂₉E₂₆) diblock copolymer micelle (aggregation number 67 based on experimental data^{13,24}) in aqueous solutions. As is seen in the cross-sectional computer simulation snapshot shown in Figure 1a at T=47°C P₂₉E₂₆ forms a well-defined mostly spherical micelle. The anisotropy of the core is rather low, 0.008 indicating shape close to a perfect sphere (Table 1). The volume

fraction distribution (Figure 1b) shows that the core contains mainly PPO and is well-separated from the PEO corona region by a relatively sharp interface of about 1 nm width (Table 1). The corona region contains well-hydrated PEO blocks.

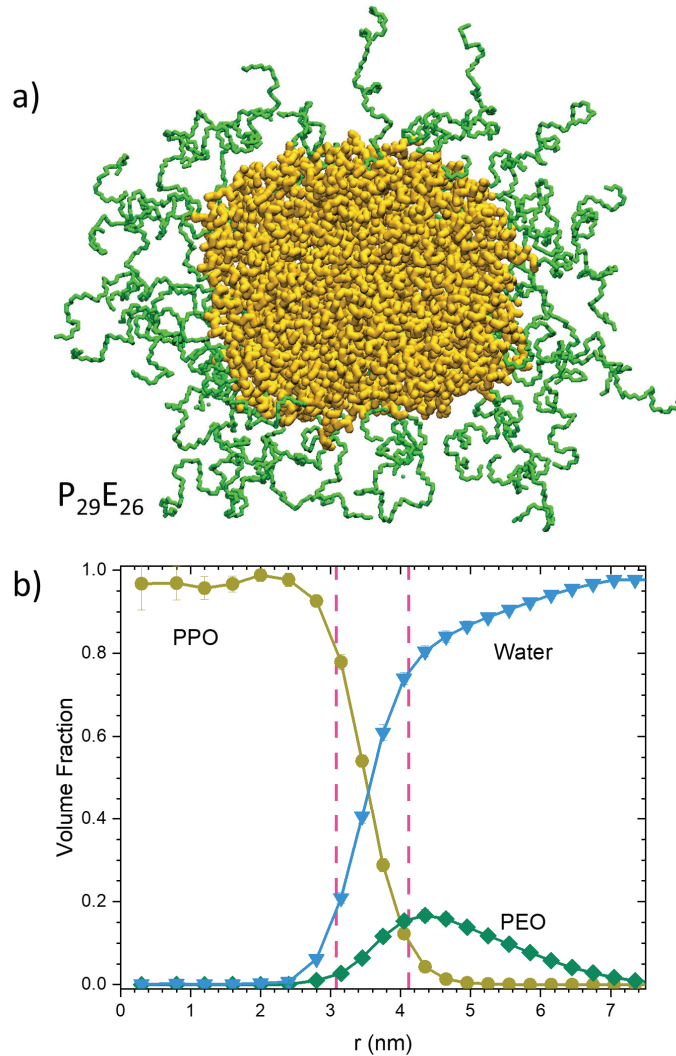


Figure 1: (a) Computer simulation snapshot (cross-sectional view) and (b) radial volume fraction profiles for PPO (yellow circles), PEO (green diamonds) and water (blue triangles) in $P_{29}E_{26}$ micelles. Vertical dashed lines indicate the interfacial region. PEO blocks are shown in green, PPO in yellow, water is not shown for clarity in the snapshot.

We have also investigated Pluronic L64 micelles formed by triblock $E_{13}P_{30}E_{13}$ with similar PPO length as in the diblock copolymer, but two twice shorter PEO blocks. For this system there have been several experimental reports of aggregation numbers from 40 to 225,^{19,23-26} so we studied three aggregation numbers: 40, 50 and 76. The results are shown in Figure 2. For all aggregation numbers of this triblock copolymer we observe the presence of water within the core: for the smaller aggregation number (40) water is distributed throughout the core, at the intermediate aggregation number (50) water is localized closer to the center and at the highest aggregation number both water and the PEO block are present in the core in the immediate vicinity of the interface (Figure 2). Furthermore, the shape of the micelles is rather irregular with the asphericity ranging between 0.08 and 0.1 with considerable interpenetration of PPO and PEO blocks within the broad interface of 1.5-1.8nm thickness (Table 1). The PEO corona is rather narrow with a noticeable fraction of the PEO chains present within the interface as well as some fraction of PPO chains that reside in the corona region (Figure 2). In this case, the core is obviously not shielded by the corona from the surrounding solution.

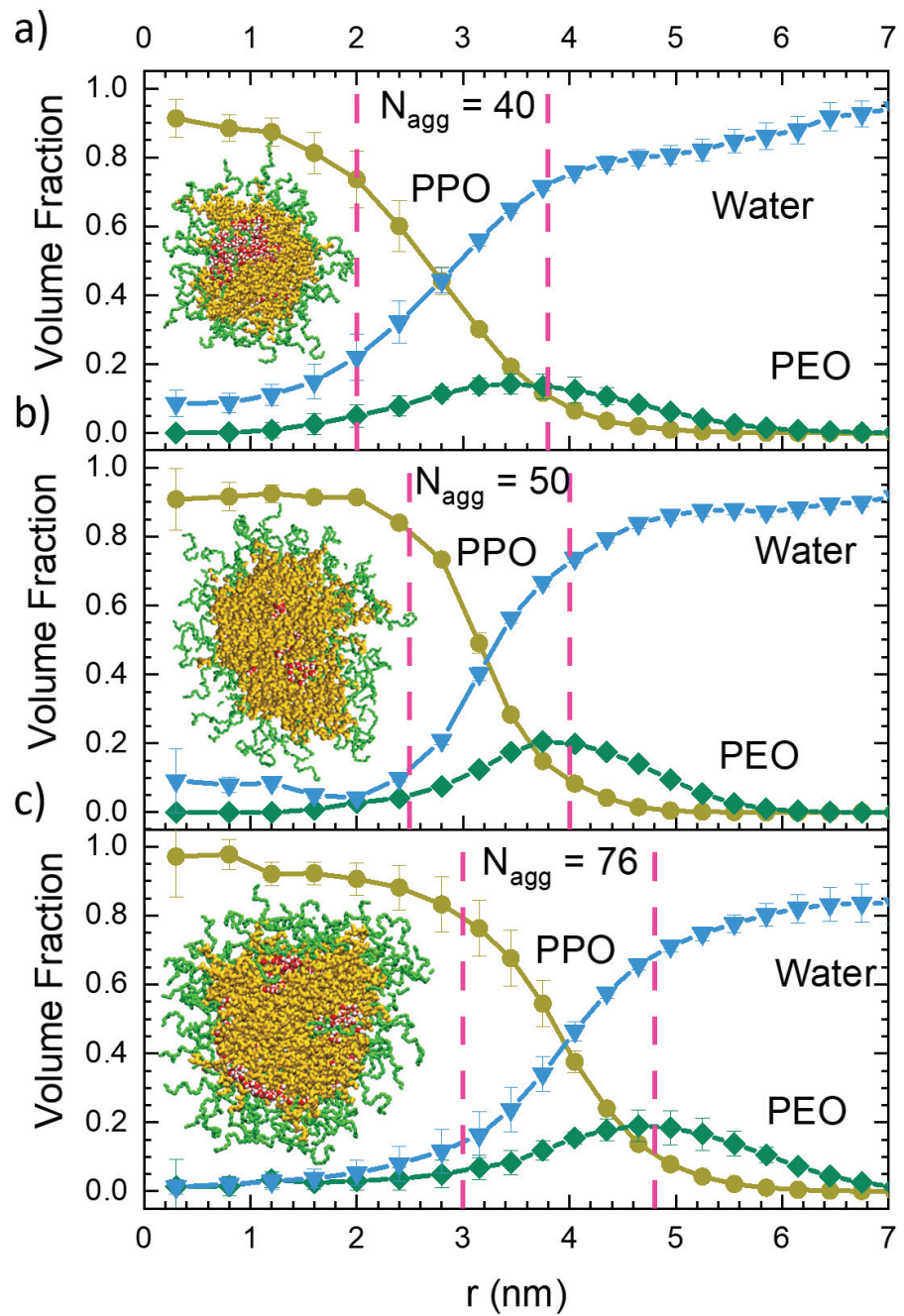


Figure 2: Computer simulation snapshots (cross-sectional view) and radial volume fraction profiles for PPO (yellow circles), PEO (green diamonds) and water (blue triangles) of Pluronic L64 (E₁₃P₃₀E₁₃) of different aggregation numbers: 40 (a), 50 (b) and 76(c). Vertical dashed lines indicate the interfacial region. In the inset snapshots PEO blocks are shown in green, PPO in yellow, water (red-and-white) is shown only within the core for clarity.

It is also informative to compare the Pluronic L64 ($E_{13}P_{30}E_{13}$) micelle structural properties to the reverse Pluronic 17R4 ($P_{14}E_{24}P_{14}$), which contains a similar PEO block length as the $P_{29}E_{26}$ diblock and twice shorter PPO blocks and forms rather small micelles with an aggregation number around 10.^{25,52} One could expect a rather ill-defined micelle with significant solvent presence in the core, but this is not the case (Figure 3). We observe practically no water in the inner region of the core. The interface is relatively broad for the micelle size, ~1nm, but more well-defined than in the L64 case and the corona is narrow, therefore providing little shielding of the core from contacts with solvent, as expected.

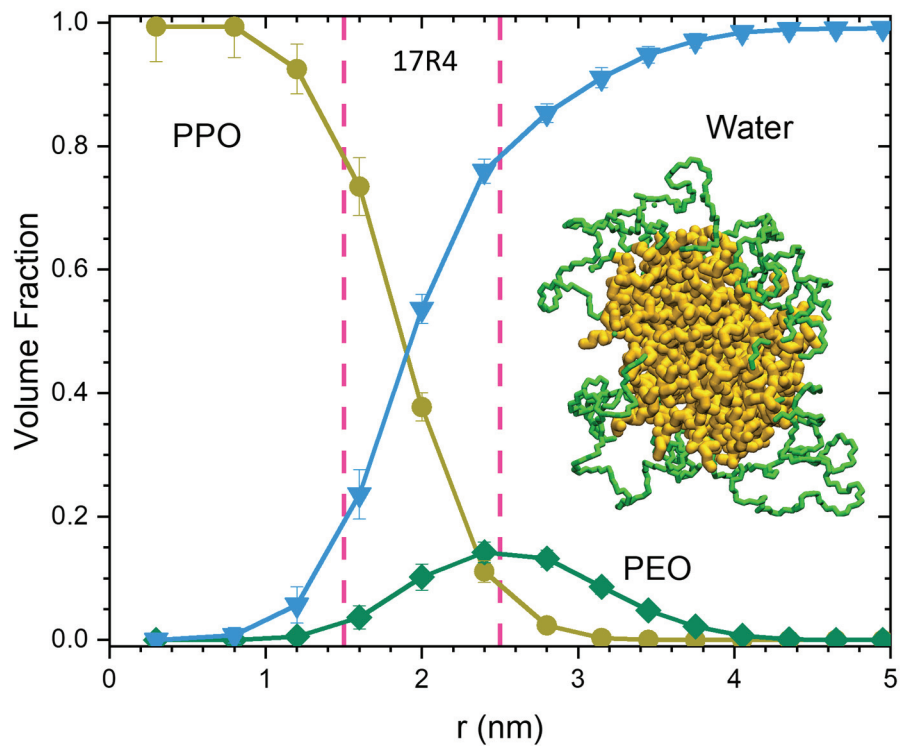


Figure 3: Computer simulation snapshots (cross-sectional view) and radial volume fraction profiles for PPO (yellow circles), PEO (green diamonds) and water (blue triangles) of reverse Pluronic 17R4 ($P_{14}E_{24}P_{14}$). Vertical dashed lines indicate the interfacial region. In the inset snapshot PEO blocks are shown in green, PPO in yellow, water is not shown for clarity.

To compare the structural properties of the micelles numerically we have calculated the radial distribution of the junction points (taken as the PPO carbon closest to the PPO-PEO junction) shown in Figures S1 and S2 of Supporting Information. The distributions have been fitted by a Gaussian function with the maximum corresponding to the core boundary and the width at the half maximum was taken as the interfacial width (with the lower boundary considered as the borderline of the inner core and the upper one as the beginning of the corona region). The values obtained for the core radius and interfacial width are shown in Table 1. As is seen the diblock copolymer micelle $P_{29}E_{26}$ has the largest core (~ 3.6 nm radius) and the narrowest interface (~ 1 nm). Depending on the aggregation number, L64 has a core radius ranging from 2.9 (for $N_{agg}=40$) to 3.9nm for ($N_{agg}=76$) with wider interfaces, 1.5-1.8nm and higher core anisotropy, while the 17R4 ($P_{14}E_{24}P_{14}$) micelle has the smallest core of about 2.0nm. It is also informative to compare the average radius of gyration for the blocks and chains in these micelles. Compared to the diblock copolymer, the PPO block and the chain overall in L64 ($E_{13}P_{30}E_{13}$) micelles have smaller R_g values (Table 1) consistent with the bent PPO block conformation within the core. Similarly, the radius of gyration of the PEO block and the overall chains are smaller in the 17R4 ($P_{14}E_{24}P_{14}$) micelle than in the diblock copolymer $P_{29}E_{26}$ micelle, which reflects the fact that the 17R4 triblock copolymer assumes hairpin conformation.⁵³

Table 1. The core radius and interface width obtained using Gaussian fitting of junction point distribution (supporting information, Figures S1 and S2), core anisotropy (eq. 1), radius of gyration for blocks and the overall chain and estimated micelle size for different micelles.

Micelle	Core Radius (nm)	Interface Thickness (nm)	Core Anisotropy	PPO Rg (nm)	PEO Rg (nm)	Chain Rg (nm)	micelle size ^a (nm)
P ₂₉ E ₂₆	3.6	1.04	0.008	1.14±0.19	1.13±0.25	1.88±0.43	7.0
L64 (N _{agg} = 40)	2.9	1.8	0.078	1.04±0.18	0.87±0.18	1.59±0.37	6.0
L64 (N _{agg} = 50)	3.25	1.5	0.076	1.06±0.18	0.83±0.15	1.60±0.37	6.0
L64 (N _{agg} = 76)	3.9	1.8	0.103	1.08±0.19	0.81±0.15	1.63±0.38	7.0
17R4	2.0	1.0	0.067	0.80±0.14	0.93±0.20	1.37±0.31	4.0

^a Estimated based on volume fraction distributions in Figures 1-3.

To gain additional insights into the block interpenetration and solvent distribution within the micelle, we calculated the volume fraction of water and each block within the inner core, interface and corona (Table 2). Comparing different micelles, we can notice that for the diblock copolymer micelle P₂₉E₂₆ and reverse Pluronic 17R4, PPO occupies about 95% of the core volume with about 5% of water present mainly near the interfacial region. In contrast, in Pluronic L64, depending on the aggregation number, PPO occupies 80-90% of the core volume with about 18-10% of water that is present mainly within the inner core. For instance for L64 with aggregation number 40, there is 18% (by volume) of water in the core in agreement with experimental data by Alexandridis.²⁶ In all cases the fraction of PEO in the core is less than 1% by volume, except for L64 with N_{agg}=76, where the volume fraction of PEO reaches 4% by volume. In the interfacial region, both PPO and PEO blocks and water are present. PEO occupies only about 10-17% of the interfacial region volume with the largest participation of PEO observed for the L64 triblock copolymer micelles with N_{agg}=76. The PPO fraction in the interfacial region ranges between 23-40% (by volume), while the water content is about 50-60% of volume with

the largest fraction in L64 triblock copolymer micelles with $N_{agg}=76$. The shell region is predominantly filled by water (~90% of volume) with 8-9% of PEO and 1-3% of PPO (by volume) in all cases.

We have also performed additional simulations of $P_{29}E_{26}$, Pluronic L64 (with aggregation number 50) and reverse Pluronic 17R4 at 37°C, where the polymer solubility in water improves. The results are shown in the Supporting Information, Figure S3. As is seen at 37°C the changes in the micelle structure for diblock copolymer and 17R4 micelles are rather minor, while the L64 micelle shape becomes even less regular with more water in the center and larger penetration of PEO block within the core.

Co-solvent effect. We have also investigated the initial stage of co-solvent interactions with $P_{29}E_{26}$, Pluronic L64 and reverse Pluronic 17R4 micelles in mixed aqueous solutions. Following experimental reports on the different influence of alcohols (depending on alkane length) on micelle stability (critical micelle temperature or concentration),^{31,32,54} we analyzed the structural properties of $P_{29}E_{26}$ micelles obtained after 130ns of equilibration in mixed aqueous solutions following homogeneous addition of 5% (by volume) of ethanol, butanol or hexanol to equilibrated micelle aqueous solutions. The results are shown in Figure 4. As is seen, overall the micelle properties have not dramatically changed. Indeed, simulation snapshots and volume fraction profiles (as well as junction point distribution, Figure S4 of supporting information) demonstrate that the micelle retains a spherical shape and does not change its size. Alcohol is mostly present at the core-corona interface and the amount consistently increases from ethanol to hexanol (Figure 4). According to Table 2, the presence of co-solvent in the interfacial zone increases from

5% (by volume) for ethanol, to 9% for butanol and 15% for hexanol. Interestingly, the total presence of water plus co-solvent remains at about 50% (by volume) similar to pure aqueous solution (Table 2). The presence of PEO at the interface slightly decreases from 10% of volume in pure water to 7-8% in mixed alcohol/water solutions, while the fraction of PPO accordingly slightly increases from 39% to 42% of volume. As to the core, the ethanol presence in the core is rather minor (ca. 1%), butanol is somewhat higher (ca. 4% of volume) and the hexanol presence is more substancial, (10% of volume) (Figure 4 and Table 2). This is not suprising as the solubility of alcohols in water noticeably decreases with an increase in alkane length ⁵⁵. The total presence of solvent (water + alcohol) in the core of the P₂₉E₂₆ micelle increases from, 4.5% of volume in pure water to 5.5% in ethanol/water solvent, to 8% in butanol/water solvent and to 13% of volume in hexanol/water solvent. In the latter case the fraction of water in the core is minimal, about 3% of volume.

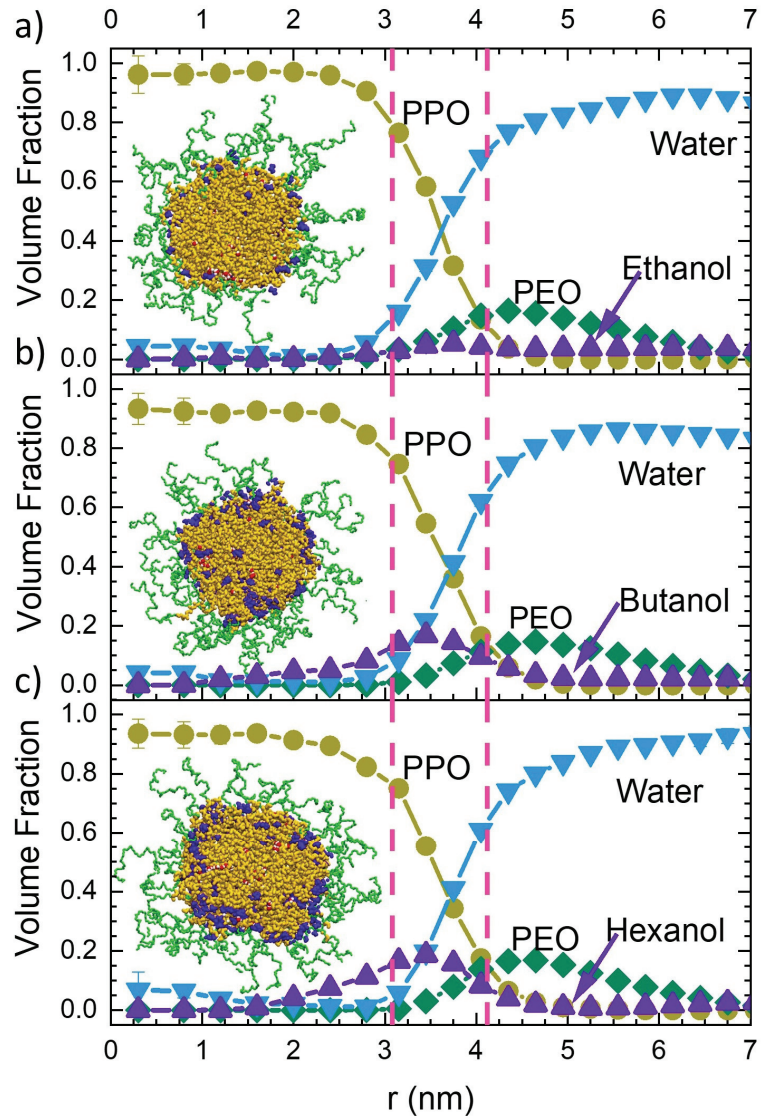


Figure 4: The radial volume fraction profiles for PPO (yellow circles), PEO (green diamonds), water (blue triangles) and alcohol (purple up triangles): ethanol (a), butanol (b) and hexanol (c) in $P_{29}E_{26}$ diblock copolymer micelles in mixed aqueous solution containing alcohol (5% by volume) after 130ns equilibration. Vertical dashed lines indicate the interfacial region. Computer simulation snapshots (cross-sectional view) of $P_{29}E_{26}$ diblock copolymer micelles with alcohol within the micelle core are shown as insets of the corresponding graphs. PEO blocks are shown in green, PPO in yellow, alcohols in purple and water is not shown for clarity.

Besides alcohol as a co-solvent, we have also investigated (within first 130ns period after co-solvent addition) $P_{29}E_{26}$ micelles in mixed aqueous solution containing 5% (by volume) glycine or isobutyric acid (IBA). These molecules contain carboxylic acid, which is capable of hydrogen bonding with PEO and PPO,^{38,39} but they differ in their solubility in water. Glycine is very soluble in water and has a relatively weak interaction with the $P_{29}E_{26}$ micelle forming hydrogen bonds with about 4-6% of oxygens of PPO and PEO. As is seen in Figure 5, glycine is present primarily at the interface (12% by volume) and slightly penetrates into the core (4%). IBA is less soluble in water, but at the composition considered IBA and water form a homogeneous solution.^{39,56} Being amphiphilic like PPO and capable of hydrogen bonding with PPO, IBA prefers to be in the micelle core (Figure 5) forming hydrogen bonds with 10% of all PPO oxygens. In the $P_{29}E_{26}$ micelle IBA is nearly homogeneously distributed throughout the core with some enhancement near the core-corona interface (Figure 5b). Overall, IBA occupies 33% (by volume) of the core of $P_{29}E_{26}$ micelles resulting in a 1.2 time increase of the core radius (Table 2). We note that the volume fraction of water within the core remains minor, 0.025. Furthermore, IBA occupies 21% (by volume) of the interfacial region bringing the total fraction of the solvent (water +IBA) to 64% of volume compared to ~50% of volume in pure aqueous solution. Accordingly, the fraction of PPO decreases from 39% to 23% of volume and the PEO slightly increases from 10% to 13%. Thus, comparing glycine and IBA interactions with $P_{29}E_{26}$ micelle one can see that more hydrophobic IBA has stronger tendency to penetrate and swell the core of the micelle. A somewhat similar trend is seen for alcohol with an increase of hydrophobicity (Figure 4), but the extent of IBA interpenetration in the core is more significant, most likely due to favorable hydrogen bonding interactions with PPO.

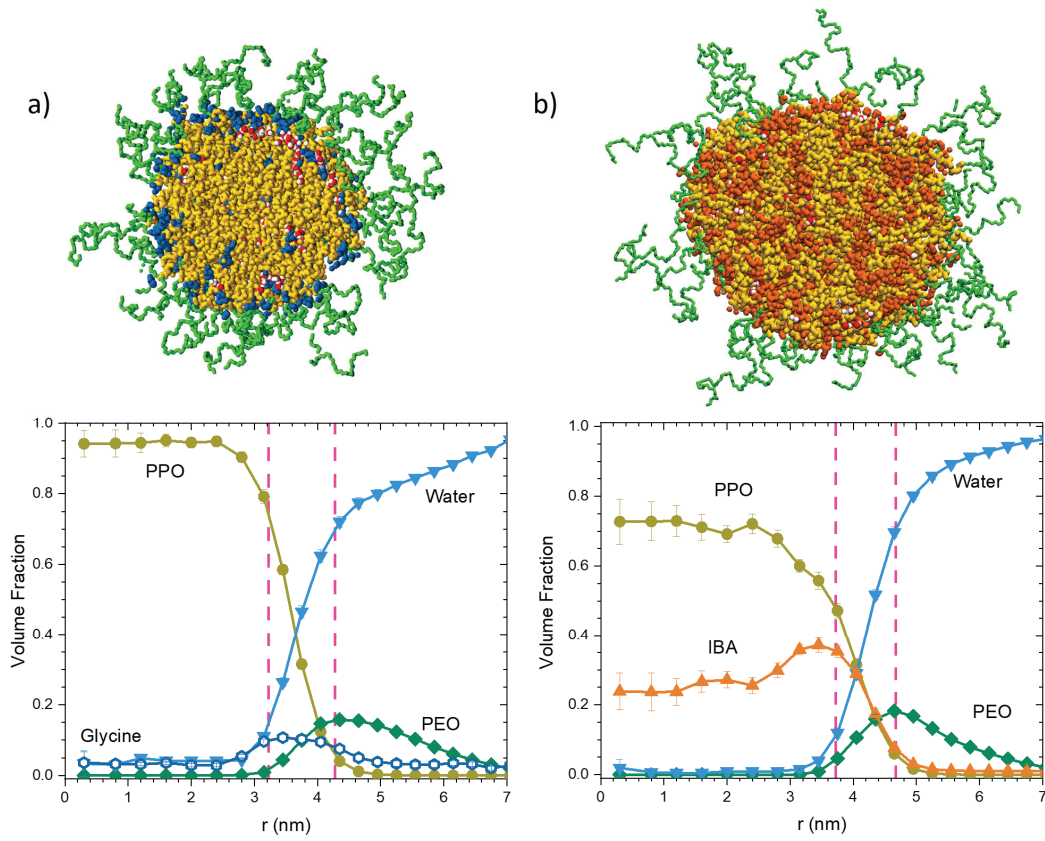


Figure 5: Computer simulation snapshots (cross-sectional view) and the radial volume fraction profiles for PPO (yellow circles), PEO (green diamonds), water (blue down triangles) and (a) glycine (open hexagons) and (b) isobutyric acid (orange up triangles), in $P_{29}E_{26}$ diblock copolymer micelles after 130ns equilibration. In the snapshots PEO blocks are shown in green, PPO in yellow, glycine in blue, IBA in orange and water (red-and-white) is shown only within the core for clarity.

It is also informative to consider the effect of alcohols (ethanol, butanol) on Pluronic L64 and reverse Pluronic 17R4 micelles. The volume fraction distributions for PPO, PEO block, water and co-solvent for L64 micelles with aggregation numbers of 50 and 76 are shown in Figure 6 together with the micelle snapshots. As is seen for Pluronic L64 the presence of alcohol makes micelle shape more spherical (cf. Figure 2 and Figure 6) and

also changes the distribution of solvent in the core. Indeed, for L64 micelle with aggregation number 50 in aqueous solution 8-10% of water is distributed within the core volume. In contrast, in the presence of ethanol or butanol (5% by volume) in solution we observe penetration of co-solvent into the core center, especially butanol, and enhancement of water in the micelle core center (Figure 6 a, b). As is seen from Table 2, about 9% by volume of butanol is present in the micelle core and the fraction of water (~8%) remains the same as in pure aqueous solution, but now it is located together with butanol in the core center. The overall presence of solvent (water + butanol) in the micelle core nearly doubles compared to water in pure aqueous solution and furthermore, it is concentrated in the core center. Furthermore, an additional 10% of butanol (by volume) is present at the core-corona interface where it replaces water while the overall fraction of solvent (water + butanol) remains close to 50% of volume similar to what we observed for P₂₉E₂₆ diblock copolymer micelles. Interestingly, in L64 micelles with aggregation number 76 (Figure 6c,d), there is a rather minor redistribution or enhancement of water within the core, but we observe some enhancement of interpenetration of PEO within the core together with alcohol. On one hand, the overall effect of butanol can be viewed as somewhat stabilizing due to the presence of the hydrophobic alkane tails at the core center and interface that helps the micelles to achieve a more regular spherical shape. On the other hand, alcohols exploit and enhance existing “defects” in these micelles, i.e. redistribute water to the core center (for smaller aggregation number) or enhance PEO content in the micelle core (for the larger aggregation number).

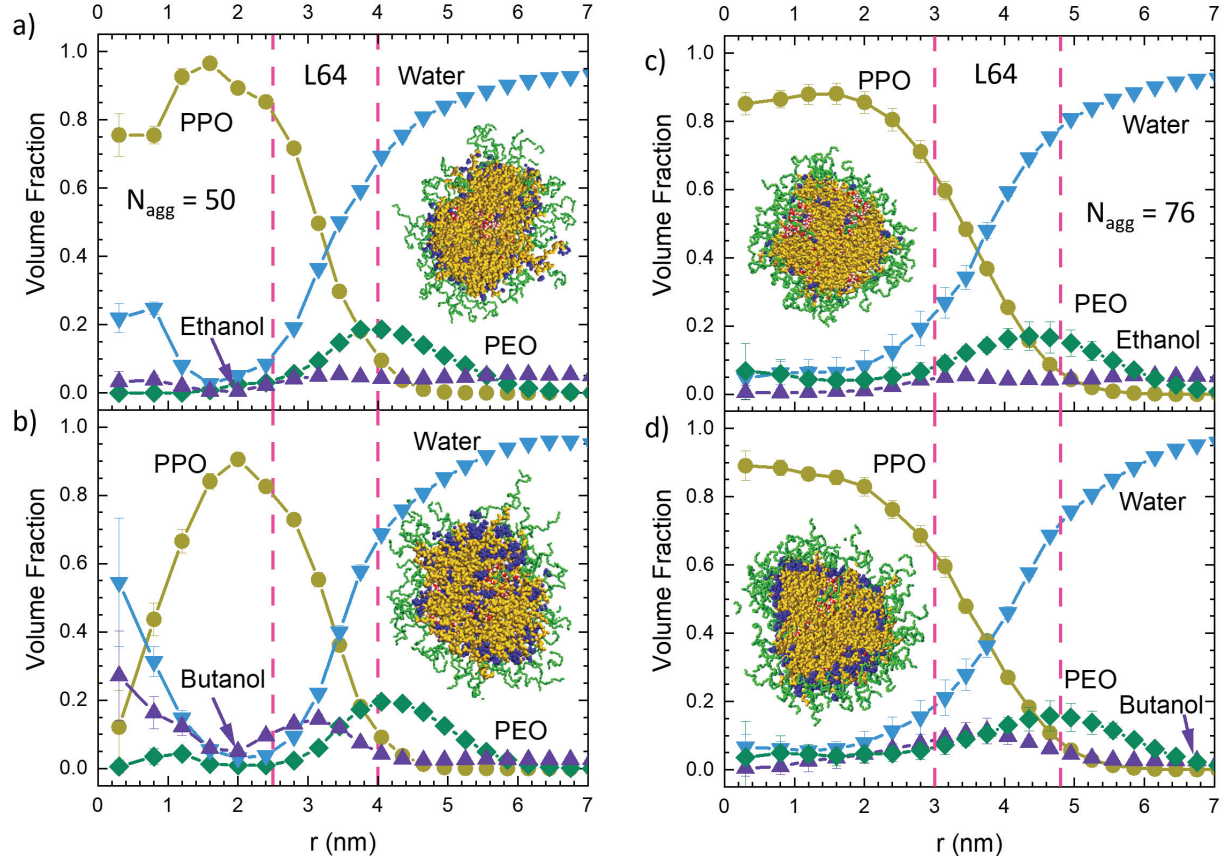


Figure 6: The radial volume fraction profiles for PPO (yellow circles), PEO (green diamonds), water (blue triangles) and alcohol (purple up triangles): ethanol (a), butanol (b) in Pluronic L64 triblock copolymer micelles with aggregation number 50 and ethanol (c), butanol (d) in Pluronic L64 triblock copolymer micelles with aggregation number 76 in mixed aqueous solution containing alcohol (5% by volume). Vertical dashed lines indicate the interfacial region. Computer simulation snapshots (cross-sectional view) of L64 micelles with alcohol within the micelle core are shown as insets of the corresponding graphs. PEO blocks are shown in green, PPO in yellow, alcohols in purple and water is not shown for clarity in the snapshots.

Table 2. Volume fraction of PPO, PEO, water and co-solvent within the core and the interface of $P_{29}E_{26}$, L64 (of different aggregation numbers) and 17R4 micelles in mixed aqueous solutions containing 5% (by volume) of co-solvent.

Micelles	Solvent	Inner core (nm)	Fraction in the Core			Interface (nm)	Fraction in the Interface			
			PPO	Water	Co-solv ent		PPO	PEO	Water	Co-solv ent
P29-E26	Water	3.08	0.95	0.045	-	1.04	0.39	0.10	0.51	-
	+ Ethanol	3.08	0.93	0.054	0.01	1.04	0.42	0.08	0.45	0.05
	+ Butanol	3.08	0.92	0.038	0.04	1.04	0.40	0.07	0.44	0.09
	+ Hexanol	3.08	0.87	0.03	0.10	1.04	0.43	0.07	0.35	0.15
	+ IBA	3.725	0.64	0.025	0.33	0.95	0.23	0.13	0.43	0.21
	+ Glycine	3.08	0.92	0.03	0.04	1.04	0.42	0.08	0.38	0.12
L64 ($N_{agg} = 40$)	Water	2.0	0.78	0.18	-	1.8	0.31	0.12	0.57	-
L64 ($N_{agg} = 50$)	Water	2.5	0.90	0.08	-	1.5	0.37	0.15	0.48	-
	+ Ethanol	2.5	0.89	0.07	0.02	1.5	0.39	0.13	0.43	0.05
	+ Butanol	2.5	0.81	0.08	0.09	1.5	0.42	0.10	0.37	0.11
L64 ($N_{agg} = 76$)	Water	3.0	0.80	0.16	-	1.8	0.23	0.17	0.60	-
	+ Ethanol	3.0	0.79	0.14	0.02	1.8	0.24	0.16	0.55	0.05
	+ Butanol	3.0	0.76	0.12	0.07	1.8	0.25	0.14	0.51	0.10
17R4	Water	1.5	0.934	0.06	-	1	0.34	0.10	0.56	-
	+ Ethanol	1.5	0.94	0.06	0	1	0.35	0.06	0.55	0.04
	+ Butanol	1.5	0.79	0.054	0.15	1	0.34	0.08	0.48	0.10
	+ Hexanol	2.3	0.41	0.06	0.53	1	0.13	0.06	0.5	0.3

For reverse Pluronic 17R4 micelles addition of alcohol (5% by volume) to aqueous solution resulted in similar, but somewhat more noticeable effects. The volume fraction distributions for PPO, PEO block, water and co-solvent together with the micelle snapshots for reverse Pluronic 17R4 micelles are shown in Figure 7. As is seen the presence of ethanol (5% by volume) in solution has a rather minor impact on the 17R4 micelle core (no ethanol present) or interface (4%), as ethanol mainly remains in the corona region and solution (Figure 7a and Table 2). In contrast, butanol propagates throughout the small micelle core contributing 15% of the core volume and bringing the total fraction of solvent in the core to 20%. There is also about 10% of butanol present at the interface. All together butanol results in some destabilization of the micelle as we observe 2 of the 10 chains separate from the core of the micelle (Figure 7b). Interestingly, addition of 5% by volume of the less water soluble hexanol to aqueous solution results in formation of a large spherical droplet of hexanol dominating the core, while the reverse Pluronic plays the role of stabilizer (Figure 7c). The overall micelle size increases with the inner core radius reaching 2.3nm compared to 1.5nm in pure aqueous solutions. Hexanol occupies 53% (by volume) of the core and 30% of the interface. As is seen, the presence of a more hydrophobic alcohol in solution results in an increase of micelle size for 17R4 reverse Pluronic in agreement with experimental observations.^{29,31} This increase is primarily due to co-solvent encapsulation within the micelle, rather than the result of micelle stabilization as is seen for reverse Pluronic the co-solvent may actually destabilize the small micelle. Thus, the effect of alcohol addition is less straightforward than in the more stable diblock copolymer micelles (Figure 4).

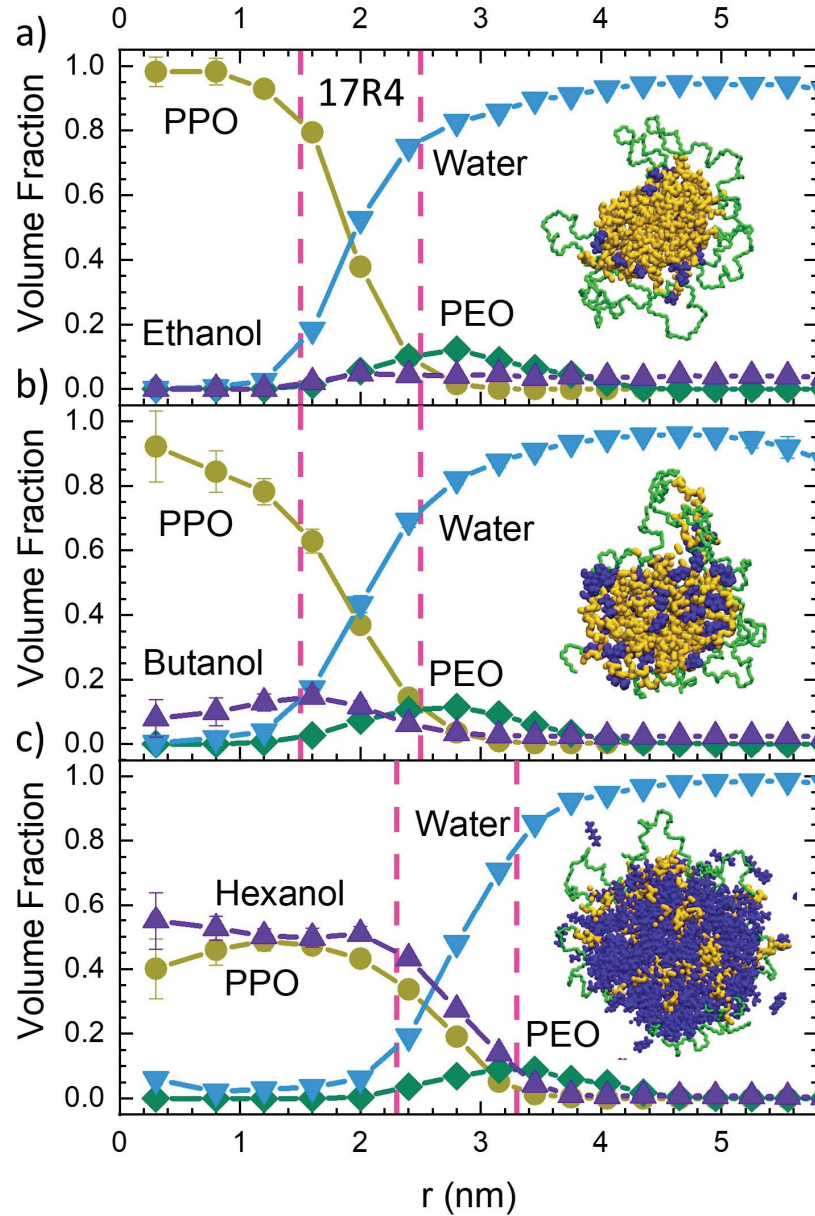


Figure 7: The radial volume fraction profiles for PPO (yellow circles), PEO (green diamonds), water (blue triangles) and alcohol (purple up triangles): ethanol (a), butanol (b) and hexanol (c) in reverse Pluronic 17R4 micelles in mixed aqueous solution containing alcohol (5% by volume). Vertical dashed lines indicate the interfacial region. Computer simulation snapshots (cross-sectional view) of 17R4 micelles with alcohol within the micelle core are shown as insets of corresponding graphs. PEO blocks are shown in green, PPO in yellow, alcohols in purple and water is not shown for clarity in the snapshots.

To investigate the stability of co-solvent and water within the micelle cores, we have analyzed how quickly solvent molecules are replaced within the core. To this end we selected solvent within the core at a given time and monitored the fraction of these solvent molecules remaining in the core at time t , $C(t)$, eq.2. The results for butanol and water within the core of L64 Pluronic with aggregation number 50 and 17R4 inverse Pluronic micelles are shown in Figure 8. As is seen water exchange occurs very quickly in 17R4 micelles with effective exchange time of 0.3ns (Table S2 of Supporting Information) and nearly all water is exchanged within 2ns. This is not surprising as micelle size is small and water is located near the interface (Figure 7b). Butanol exchange occurs more slowly with effective exchange time of about 2.4ns (Table S2 of Supporting Information): about 1/3 remains in the core after 4ns. Obviously, the butanol molecule is larger than water, so it diffuses more slowly plus butanol is spread throughout the core with a relatively small fraction present in the corona region of the 17R4 micelle. In contrast, in the L64 micelle (with aggregation number 50) water and butanol exchange occurs more slowly than in 17R4 micelle: more than 60% of the original solvent remains within the core after 4ns. The L64 micelle is larger in size and furthermore the solvent is localized near the core center, as shown in Figure 8a (and Figure 6b) making exchange particularly slow. Water exchange in the presence of butanol occurs much slower (effective decay time of about 4ns, Table S2 of Supporting Information) than in the same L64 micelle in pure water (effective exchange time of about 1ns, Table S2 of Supporting Information). In the presence of butanol water is localized closer to the micelle center, while in L64 micelle in pure aqueous solution water is more homogeneously distributed throughout the core, facilitating water exchange between the interface and corona regions. The likely reason

for significant slowing down of the water exchange in the presence of butanol is that molecular transport occurs collectively. As is seen in Figure 8a, there is co-localization of butanol and water within the core and a channel forms between the inner water pool and interface, along which both water and butanol travel. Another interesting observation is the butanol hydroxyl group orientation towards the nearby water. For butanol located at the interface its orientation is either radial with hydroxyl groups located at the interface and alkane tails within the core or along the core surface. In both cases this allows hydrogen bonding with water for the hydroxyl groups and interaction with PPO for the alkane tails. This is consistent with experimental results by Parekh et al. who concluded based on NMR results that the hydroxyl group of the alcohol co-localized near the PEO at the interface, while the methyl tail of longer alcohols is located in the micelle interior.^{31,32} As is seen from Figure 8a for the butanol located closer to the L64 micelle core the orientation can also be radial but with hydroxyl groups oriented towards the core center and located in the water pool, while alkane tails remain in the PPO vicinity.

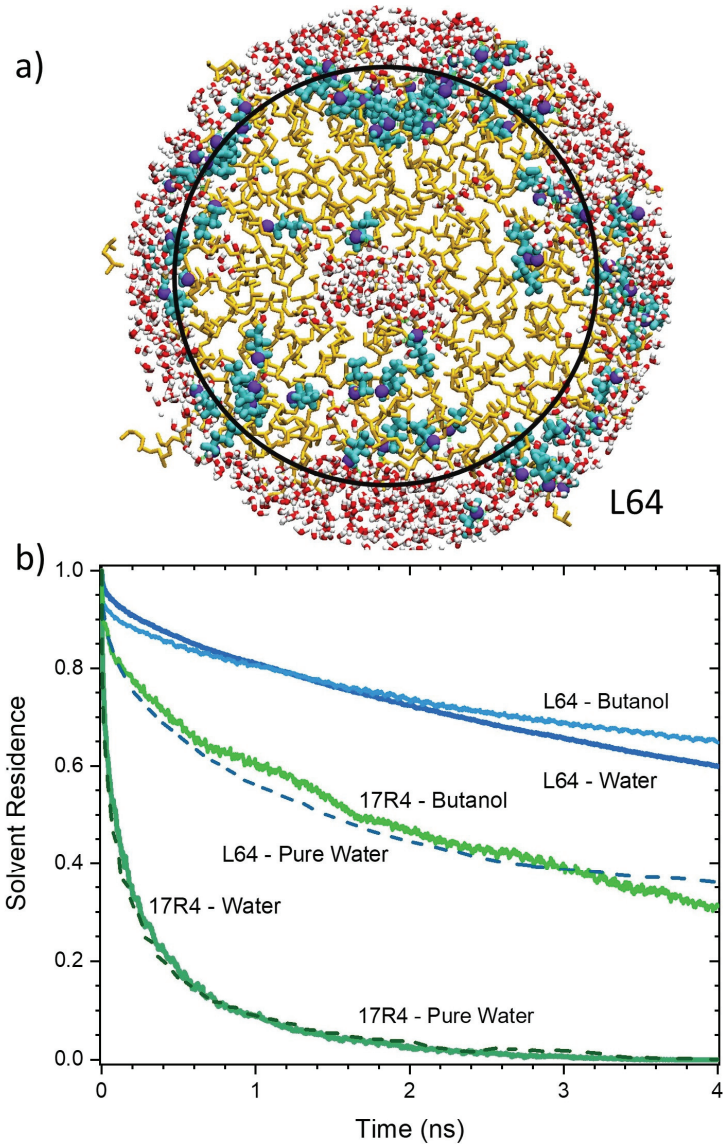


Figure 8: a) Computer simulation snapshot (cross-sectional view) of the core of L64 triblock copolymer micelle with aggregation number 50 (inner area is circled) showing water (red and white) and butanol (cyan with hydroxyl group in purple), PPO block is shown in yellow, PEO blocks and the micelle corona are not shown. (b) The fraction of solvent (water or butanol) remaining within the inner core of Pluronic L64 triblock copolymer micelle with aggregation number 50 (blue curves) and reverse Pluronic 17R4 micelles (green curves) as a function of time in mixed aqueous solution containing (5% by volume) butanol (solid curves) in comparison to time dependence for the water residence in L64 (with $N_{agg}=50$) and in 17R4 in pure aqueous solutions (dashed curves).

Conclusions.

Using atomistic molecular dynamics simulations we investigated and compared the structure of P₂₉E₂₆ diblock copolymer micelles, Pluronic L64 and reverse Pluronic 17R4 micelles formed by monodisperse diblock and triblock copolymers of similar length but with different distributions of PPO and PEO blocks in pure aqueous solution and or with added co-solvents. For the case of L64 Pluronic we also considered the impact of micelle aggregation number, which so far as we know has not been done in previous simulation studies. In pure aqueous solutions we found that P₂₉E₂₆ diblock copolymer micelles and reverse Pluronic 17R4 micelles form well-defined spherical micelles with a negligible amount of water present in the inner micelle cores (Figures 1 and 3). In contrast, the shape of Pluronic L64 micelles is not perfectly symmetric and the core contains about 10-18% of water (by volume) either distributed throughout the core for L64 micelles with smaller aggregation numbers (N_{agg}=40,50) or localized closer to the interface for the larger aggregation number (N_{agg}=76) (Figure 2, Table 1) in agreement with previous computer simulation and experimental results.^{7,8,26,57} Accordingly, L64 micelles have broader interface, where PPO, PEO and water are all present (Figure 2). The observed differences in micelle structure, which are consistent with earlier experimental observations^{13,24} reflect the PPO packing in diblock or reversed PPO-PEO-PPO Pluronics where the PPO block(s) have a nearly straight (linear) conformation in the core, while for the PEO-PPO-PEO Pluronics the PPO assumes a bent conformation. The PPO block bending and interpenetration of PEO and water in the core result in a non-spherical micelle shape for L64 compared to a PPO-PEO diblock copolymer micelle. These differences in micelle structure have important implications for micelle stability and

applications e.g. in drug delivery. For example, the presence of water in the micelle core may not be desirable for e.g., hydrolysable drug delivery, and the broad interface may result in poor shielding of the core that can compromise micelle longevity during the drug delivery process.

The influence of co-solvents (5% by volume) on micelle properties during the first 130 ns after their introduction has been investigated and the results for diblock and triblock copolymer micelles are compared. We found that in all cases ethanol does not penetrate the micelle core but is located mainly at the core-corona interface (Figure 4, 6, 7, Table 2). For L64 micelles the presence of ethanol at the interface stimulated re-distribution of water within the core towards the center (for the smaller aggregation number $N_{agg}=50$) or enhanced PEO interpenetration to the core (for the larger aggregation number $N_{agg}=76$) (Figure 6). With an increase of alcohol hydrophobicity the extent of co-solvent penetration into the core and the interface increased for all micelles (Figure 4, 6, 7, Table 2). For the diblock copolymer micelle alcohol penetration is accompanied by a decrease in water within the core and at the interface, while in triblock copolymers the presence of co-solvent does not necessarily result in a decrease of incorporated water. We found that a long-tail alcohol orients its hydroxyl group towards the water, i.e. in the interfacial region while the alkane tails are directed towards the center in agreement with experimental expectations^{31,32} or along the interface to maintain hydrogen bonding with water. However, within the micelle core the orientation may be reversed in the vicinity of water pool at the core center (Figure 8). Furthermore, for the reverse 17R4 Pluronic we observed that butanol insertion into the core of this small micelle resulted in chain

extraction from the core, i.e. caused some destabilization of the micelle (Figure 7) while hexanol causes swelling of the micelle core. In contrast to alcohols that have a rather weak propensity to form hydrogen bonds with PEO or PPO, glycine and especially isobutyric acid (IBA) more actively form hydrogen bonds with PPO (and to a lesser extent with PEO) and their incorporation resulted in more dramatic micelle changes for the diblock copolymer micelle. Significant encapsulation of IBA is observed in the core (occupying 33% of volume) resulting in swelling of the PPO core and an increase of the core size by 1.2 times (Figure 5). IBA penetration into the core was accompanied by water escape. Our results on the initial structural changes of the micelles in the presence of co-solvents provide insights on the propensity of co-solvent penetration and the effect of co-solvent on the amount of water present in the micelle core and interface. These results provide useful insights in the interpretation of experimental data and practical applications of PPO-PEO micelles and Pluronics in solubilization and drug delivery.

ASSOCIATED CONTENT

Supporting Information:

The Supporting Information is available free of charge at <https://pubs.acs.org/doi/10.1021/acs.langmuir.3c03103>....

Additional computational details on micelle simulations, distributions of junction point between blocks, radial volume fraction distributions for P₂₉E₂₆, Pluronic L64, and reverse Pluronic 17R4 micelles at 37C, core radius and half-width obtained from Gaussian fitting for P₂₉E₂₆, Pluronic L64, and reverse Pluronic 17R4 micelles in aqueous solution and mixed solvents; fitting parameters of a triexponential fit for different solvent residence correlation functions.

AUTHOR INFORMATION

Corresponding Author:

Elena E. Dormidontova – Polymer Program, Institute of Materials Science and Physics Department, University of Connecticut, Storrs, Connecticut 06269, United States. Orcid: 0000-0002-7669-8957. Email: elena@uconn.edu

ACKNOWLEDGMENTS

This research is supported by the National Science Foundation under Grant No. DMR-1916864. This work used the Extreme Science and Engineering Discovery Environment (XSEDE) through allocation TG-MAT210004. XSEDE is supported by National Science Foundation grant number ACI-1548562.

References

- (1) Karimi, M.; Sahandi Zangabad, P.; Ghasemi, A.; Amiri, M.; Bahrami, M.; Malekzad, H.; Ghahramanzadeh Asl, H.; Mahdieh, Z.; Bozorgomid, M.; Ghasemi, A.; Rahmani Taji Boyuk, M. R.; Hamblin, M. R. Temperature-Responsive Smart Nanocarriers for Delivery of Therapeutic Agents: Applications and Recent Advances. *ACS Appl. Mater. Interfaces* **2016**, *8* (33), 21107–21133. <https://doi.org/10.1021/acsami.6b00371>.
- (2) Ward, M. A.; Georgiou, T. K. Thermoresponsive Polymers for Biomedical Applications. *Polymers (Basel)*. **2011**, *3* (3), 1215–1242. <https://doi.org/10.3390/polym3031215>.
- (3) Pitt-Barry, A.; Barry, N. P. E. Pluronic® Block-Copolymers in Medicine: From Chemical and Biological Versatility to Rationalisation and Clinical Advances.

Polym. Chem. **2014**, *5* (10), 3291–3297. <https://doi.org/10.1039/c4py00039k>.

- (4) Huang, H.-J.; Tsai, Y.-L.; Lin, S.-H.; Hsu, S. Smart Polymers for Cell Therapy and Precision Medicine. *J. Biomed. Sci.* **2019**, *26* (1), 73. <https://doi.org/10.1186/s12929-019-0571-4>.
- (5) Bodratti, A. M.; Alexandridis, P. Formulation of Poloxamers for Drug Delivery. *J. Funct. Biomater.* **2018**, *9* (1). <https://doi.org/10.3390/jfb9010011>.
- (6) Fusco, S.; Borzacchiello, A.; Netti, P. A. Perspectives on: PEO-PPO-PEO Triblock Copolymers and Their Biomedical Applications. *J. Bioact. Compat. Polym.* **2006**, *21* (2), 149–164. <https://doi.org/10.1177/0883911506063207>.
- (7) Bedrov, D.; Smith, G. D.; Yoon, J. Structure and Interactions in Micellar Solutions: Molecular Simulations of Pluronic L64 Aqueous Solutions. *Langmuir* **2007**, *23* (24), 12032–12041. <https://doi.org/10.1021/la700742z>.
- (8) Bedrov, D.; Ayyagari, C.; Smith, G. D. Multiscale Modeling of Poly(Ethylene Oxide)-Poly(Propylene Oxide)-Poly(Ethylene Oxide) Triblock Copolymer Micelles in Aqueous Solution. *J. Chem. Theory Comput.* **2006**, *2* (3), 598–606. <https://doi.org/10.1021/ct050334k>.
- (9) Samanta, S.; Roccatano, D. Interaction of Curcumin with PEO-PPO-PEO Block Copolymers: A Molecular Dynamics Study. *J. Phys. Chem. B* **2013**, *117* (11), 3250–3257. <https://doi.org/10.1021/jp309476u>.
- (10) Nawaz, S.; Carbone, P. Coarse-Graining Poly(Ethylene Oxide)-Poly(Propylene Oxide)-Poly(Ethylene Oxide) (PEO-PPO-PEO) Block Copolymers Using the MARTINI Force Field. *J. Phys. Chem. B* **2014**, *118* (6), 1648–1659. <https://doi.org/10.1021/jp4092249>.
- (11) Nawaz, S.; Redhead, M.; Mantovani, G.; Alexander, C.; Bosquillon, C.; Carbone, P. Interactions of PEO-PPO-PEO Block Copolymers with Lipid Membranes: A Computational and Experimental Study Linking Membrane Lysis with Polymer Structure. *Soft Matter* **2012**, *8* (25), 6744–6754. <https://doi.org/10.1039/c2sm25327e>.
- (12) Ileri Ercan, N.; Stroeve, P.; Tringe, J. W.; Faller, R. Understanding the Interaction of Pluronics L61 and L64 with a DOPC Lipid Bilayer: An Atomistic Molecular Dynamics Study. *Langmuir* **2016**, *32* (39), 10026–10033.

<https://doi.org/10.1021/acs.langmuir.6b02360>.

- (13) Booth, C.; Attwood, D. Effects of Block Architecture and Composition on the Association Properties of Poly(Oxyalkylene) Copolymers in Aqueous Solution. *Macromol. Rapid Commun.* **2000**, 21 (9), 501–527. [https://doi.org/10.1002/1521-3927\(20000601\)21:9<501::AID-MARC501>3.0.CO;2-R](https://doi.org/10.1002/1521-3927(20000601)21:9<501::AID-MARC501>3.0.CO;2-R).
- (14) Nagarajan, R. Solubilization of Hydrocarbons and Resulting Aggregate Shape Transitions in Aqueous Solutions of Pluronic® (PEO-PPO-PEO) Block Copolymers. *Colloids Surfaces B Biointerfaces* **1999**, 16 (1–4), 55–72. [https://doi.org/10.1016/S0927-7765\(99\)00061-2](https://doi.org/10.1016/S0927-7765(99)00061-2).
- (15) Nagarajan, R.; Ganesh, K. Comparison of Solubilization of Hydrocarbons in (PEO-PPO) Diblock versus (PEO-PPO-PEO) Triblock Copolymer Micelles. *J. Colloid Interface Sci.* **1996**, 184 (2), 489–499. <https://doi.org/10.1006/jcis.1996.0644>.
- (16) Nagarajan, R.; Ganesh, K. Block Copolymer Self-Assembly in Selective Solvents: Theory of Solubilization in Spherical Micelles. *Macromolecules* **1989**, 22 (11), 4312–4325. <https://doi.org/10.1021/ma00201a029>.
- (17) Liu, T.; Nace, V. M.; Chu, B. Cloud-Point Temperatures of BnEmBn and PnEmPn Type Triblock Copolymers in Aqueous Solution. *J. Phys. Chem. B* **1997**, 101 (41), 8074–8078. <https://doi.org/10.1021/jp970813i>.
- (18) Nagarajan, R.; Ganesh, K. Block Copolymer Self-Assembly in Selective Solvents: Theory of Solubilization in Spherical Micelles. *Macromolecules* **1989**, 22 (11), 4312–4325. <https://doi.org/10.1021/ma00201a029>.
- (19) Wanka, G.; Hoffmann, H.; Ulbricht, W. Phase Diagrams and Aggregation Behavior of Poly(Oxyethylene)-Poly(Oxypropylene)-Poly(Oxyethylene) Triblock Copolymers in Aqueous Solutions. *Macromolecules* **1994**, 27 (15), 4145–4159. <https://doi.org/10.1021/ma00093a016>.
- (20) Linse, P. Micellization of Poly(Ethylene Oxide)-Poly(Propylene Oxide) Block Copolymers in Aqueous Solution. *Macromolecules* **1993**, 26 (17), 4437–4449. <https://doi.org/10.1021/ma00069a007>.
- (21) Armstrong, J.; Chowdhry, B.; O'Brien, R.; Beezer, A.; Mitchell, J.; Leharne, S. On the Molecular Origin of the Cooperative Coil-to-Globule Transition of Poly(: N-

Isopropylacrylamide) in Water. *J. Phys. Chem. B* **1998**, *102* (1), 1–6. <https://doi.org/10.1039/c8cp00537k>.

(22) Armstrong, J.; Chowdhry, B.; O'Brien, R.; Beezer, A.; Mitchell, J.; Leharne, S. Scanning Microcalorimetric Investigations of Phase Transitions in Dilute Aqueous Solutions of Poly(Oxypropylene). *J. Phys. Chem.* **1995**, *99* (13), 4590–4598. <https://doi.org/10.1021/j100013a033>.

(23) Ganguly, R.; Choudhury, N.; Aswal, V. K.; Hassan, P. A. Pluronic L64 Micelles near Cloud Point: Investigating the Role of Micellar Growth and Interaction in Critical Concentration Fluctuation and Percolation. *J. Phys. Chem. B* **2009**, *113* (3), 668–675. <https://doi.org/10.1021/jp808304w>.

(24) Yang, L.; Bedells, A. D.; Attwood, D.; Booth, C. Association and Surface Properties of Diblock and Triblock Copoly(Oxyethylene/Oxypropylene/Oxyethylene)S. *J. Chem. Soc. Faraday Trans.* **1992**, *88* (10), 1447–1452. <https://doi.org/10.1039/FT9928801447>.

(25) Zhou, Z.; Chu, B. Phase Behavior and Association Properties of Poly(Oxypropylene)-Poly(Oxyethylene)-Poly(Oxypropylene) Triblock Copolymer in Aqueous Solution. *Macromolecules* **1994**, *27* (8), 2025–2033. <https://doi.org/10.1021/ma00086a008>.

(26) Yang, L.; Alexandridis, P.; Steytler, D. C.; Kositza, M. J.; Holzwarth, J. F. Small-Angle Neutron Scattering Investigation of the Temperature-Dependent Aggregation Behavior of the Block Copolymer Pluronic L64 in Aqueous Solution. *Langmuir* **2000**, *16* (23), 8555–8561. <https://doi.org/10.1021/la000008m>.

(27) Pedersen, J. S.; Gerstenberg, M. C. The Structure of P85 Pluronic Block Copolymer Micelles Determined by Small-Angle Neutron Scattering. *Colloids Surfaces A Physicochem. Eng. Asp.* **2003**, *213* (2–3), 175–187. [https://doi.org/10.1016/S0927-7757\(02\)00511-3](https://doi.org/10.1016/S0927-7757(02)00511-3).

(28) Dahanayake, R.; Dormidontova, E. E. Hydrogen Bonding Sequence Directed Coil-Globule Transition in Water Soluble Thermoresponsive Polymers. *Phys. Rev. Lett.* **2021**, *127* (16), 167801. <https://doi.org/10.1103/physrevlett.127.167801>.

(29) Patel, V.; Dey, J.; Ganguly, R.; Kumar, S.; Nath, S.; Aswal, V. K.; Bahadur, P. Solubilization of Hydrophobic Alcohols in Aqueous Pluronic Solutions:

Investigating the Role of Dehydration of the Micellar Core in Tuning the Restructuring and Growth of Pluronic Micelles. *Soft Matter* **2013**, *9* (31), 7583–7591. <https://doi.org/10.1039/c3sm50600b>.

(30) Patidar, P.; Pillai, S. A.; Bahadur, P.; Bahadur, A. Tuning the Self-Assembly of EO-PO Block Copolymers and Quercetin Solubilization in the Presence of Some Common Pharmaceutical Excipients: A Comparative Study on a Linear Triblock and a Starblock Copolymer. *Journal of Molecular Liquids*. 2017, pp 511–519. <https://doi.org/10.1016/j.molliq.2017.06.035>.

(31) Parmar, A.; Bharatiya, B.; Patel, K.; Aswal, V.; Bahadur, P. Alkanol-Induced Micelles of a Very Hydrophilic Eo-Po-Eo Block Copolymer: Characterization by Spectral and Scattering Methods. *J. Surfactants Deterg.* **2013**, *16* (1), 105–114. <https://doi.org/10.1007/s11743-012-1365-9>.

(32) Parekh, P.; Singh, K.; Marangoni, D. G.; Bahadur, P. Effect of Alcohols on Aqueous Micellar Solutions of PEO-PPO-PEO Copolymers: A Dynamic Light Scattering and ¹H NMR Study. *J. Mol. Liq.* **2012**, *165*, 49–54. <https://doi.org/10.1016/j.molliq.2011.10.007>.

(33) Hsu, Y. H.; Tsui, H. W.; Lee, C. F.; Chen, S. H.; Chen, L. J. Effect of Alcohols on the Heat of Micellization of Pluronic F88 Aqueous Solutions. *Colloid Polym. Sci.* **2015**, *293* (12), 3403–3415. <https://doi.org/10.1007/s00396-015-3662-0>.

(34) Alexandridis, P.; Lin, Y. 5587 SANS Investigation of Polyether Block Copolymer Micelle Structure in Mixed Solvents of Water and Formamide, Ethanol, or Glycerol. *Macromolecules* **2000**, *33* (15), 5574–5587. <https://doi.org/10.1021/ma000332o>.

(35) Linse, P.; Malmsten, M. Temperature-Dependent Micellization in Aqueous Block Copolymer Solutions. *Macromolecules* **1992**, *25* (20), 5434–5439. <https://doi.org/10.1021/ma00046a048>.

(36) Aydin, F.; Chu, X.; Uppaladadium, G.; Devore, D.; Goyal, R.; Murthy, N. S.; Zhang, Z.; Kohn, J.; Dutt, M. Self-Assembly and Critical Aggregation Concentration Measurements of ABA Triblock Copolymers with Varying B Block Types: Model Development, Prediction, and Validation. *J. Phys. Chem. B* **2016**, *120* (15), 3666–3676. <https://doi.org/10.1021/acs.jpcb.5b12594>.

(37) Kacar, G. Molecular Understanding of Interactions, Structure, and Drug Encapsulation Efficiency of Pluronic Micelles from Dissipative Particle Dynamics Simulations. *Colloid Polym. Sci.* **2019**, 297 (7–8), 1037–1051. <https://doi.org/10.1007/s00396-019-04535-0>.

(38) Dahanayake, R.; Dahal, U.; Dormidontova, E. E. Co-Solvent and Temperature Effect on Conformation and Hydration of Polypropylene and Polyethylene Oxides in Aqueous Solutions. *J. Mol. Liq.* **2022**, 362, 1–12. <https://doi.org/10.1016/j.molliq.2022.119774>.

(39) Dahal, U. R.; Dormidontova, E. E. The Dynamics of Solvation Dictates the Conformation of Polyethylene Oxide in Aqueous, Isobutyric Acid and Binary Solutions. *Phys. Chem. Chem. Phys.* **2017**, 19 (15), 9823–9832. <https://doi.org/10.1039/c7cp00526a>.

(40) Towns, J.; Cockerill, T.; Dahan, M.; Foster, I.; Gaither, K.; Grimshaw, A.; Hazlewood, V.; Lathrop, S.; Lifka, D.; Peterson, G. D.; Roskies, R.; Scott, J. R.; Wilkins-Diehr, N. XSEDE: Accelerating Scientific Discovery. *Comput. Sci. & Eng.* **2014**, 16 (5), 62–74. <https://doi.org/10.1109/MCSE.2014.80>.

(41) Jorgensen, W. L.; Maxwell, D. S.; Tirado-Rives, J. Development and Testing of the OPLS All-Atom Force Field on Conformational Energetics and Properties of Organic Liquids. *J. Am. Chem. Soc.* **1996**, 118 (45), 11225–11236. <https://doi.org/10.1021/ja9621760>.

(42) Mao, Y.; Zhang, Y. Thermal Conductivity, Shear Viscosity and Specific Heat of Rigid Water Models. *Chem. Phys. Lett.* **2012**, 542, 37–41. <https://doi.org/10.1016/j.cplett.2012.05.044>.

(43) Mark, P.; Nilsson, L. Structure and Dynamics of the TIP3P, SPC, and SPC/E Water Models at 298 K. *J. Phys. Chem. A* **2001**, 105 (43), 9954–9960. <https://doi.org/10.1021/jp003020w>.

(44) Zhang, X.; Wang, Y.; Yao, J.; Li, H.; Mochizuki, K. A Tiny Charge-Scaling in the OPLS-AA + L-OPLS Force Field Delivers the Realistic Dynamics and Structure of Liquid Primary Alcohols. *J. Comput. Chem.* **2022**, 43 (6), 421–430. <https://doi.org/10.1002/jcc.26802>.

(45) Zangi, R. Refinement of the OPLSAA Force-Field for Liquid Alcohols. *ACS*

Omega **2018**, *3* (12), 18089–18099. <https://doi.org/10.1021/acsomega.8b03132>.

(46) Martínez, J. M.; Martínez, L. Packing Optimization for Automated Generation of Complex System's Initial Configurations for Molecular Dynamics and Docking. *J. Comput. Chem.* **2003**, *24* (7), 819–825. <https://doi.org/10.1002/jcc.10216>.

(47) Martínez, L.; Andrade, R.; Birgin, E. G.; Martínez, J. M. PACKMOL: A Package for Building Initial Configurations for Molecular Dynamics Simulations. *J. Comput. Chem.* **2009**, *30* (13), 2157–2164. <https://doi.org/10.1002/jcc.21224>.

(48) Zhou, Z.; Chu, B. Anomalous Micellization Behavior and Composition Heterogeneity of a Triblock ABA Copolymer of (A) Ethylene Oxide and (B) Propylene Oxide in Aqueous Solution. *Macromolecules* **1988**, *21* (8), 2548–2554. <https://doi.org/10.1021/ma00186a039>.

(49) Bondi, A. Van Der Waals Volumes and Radii. *J. Phys. Chem.* **1964**, *68* (3), 441–451. <https://doi.org/10.1021/j100785a001>.

(50) Zhao, Y. H.; Abraham, M. H.; Zissimos, A. M. Fast Calculation of van Der Waals Volume as a Sum of Atomic and Bond Contributions and Its Application to Drug Compounds. *J. Org. Chem.* **2003**, *68* (19), 7368–7373. <https://doi.org/10.1021/jo034808o>.

(51) Humphrey, W.; Dalke, A.; Schulten, K. VMD: Visual Molecular Dynamics. *J. Mol. Graph.* **1996**, *14* (October 1995), 33–38.

(52) Kumi, B. C.; Hammouda, B.; Greer, S. C. Self-Assembly of the Triblock Copolymer 17R4 Poly(Propylene Oxide)14-Poly(Ethylene Oxide)24-Poly(Propylene Oxide)14 in D2O. *J. Colloid Interface Sci.* **2014**, *434*, 201–207. <https://doi.org/10.1016/j.jcis.2014.07.049>.

(53) Patel, T.; Bahadur, P.; Mata, J. The Clouding Behaviour of PEO-PPO Based Triblock Copolymers in Aqueous Ionic Surfactant Solutions: A New Approach for Cloud Point Measurements. *J. Colloid Interface Sci.* **2010**, *345* (2), 346–350. <https://doi.org/10.1016/j.jcis.2010.01.079>.

(54) Hsu, Y. H.; Tsui, H. W.; Lee, C. F.; Chen, S. H.; Chen, L. J. Erratum to: Effect of Alcohols on the Heat of Micellization of Pluronic F88 Aqueous Solutions [Colloid Polym Sci, DOI 10.1007/S00396-015-3662-0]. *Colloid Polym. Sci.* **2015**, *293* (12), 3417. <https://doi.org/10.1007/s00396-015-3766-6>.

(55) Kinoshita, K.; Ishikawa, H.; Shinoda, K. Solubility of Alcohols in Water Determined the Surface Tension Measurements. *Bull. Chem. Soc. Jpn.* **1958**, *31* (9), 1081–1082. <https://doi.org/10.1246/bcsj.31.1081>.

(56) Colombani, J.; Bert, J. Early Sedimentation and Crossover Kinetics in an Off-Critical Phase-Separating Liquid Mixture. *Phys. Rev. E - Stat. Physics, Plasmas, Fluids, Relat. Interdiscip. Top.* **2004**, *69* (1), 6. <https://doi.org/10.1103/PhysRevE.69.011402>.

(57) Brown, W.; Schillen, K.; Almgren, M.; Hvidt, S.; Bahadur, P. Micelle and Gel Formation in a Poly(Ethylene Oxide)/Poly(Propylene Oxide)/Poly(Ethylene Oxide) Triblock Copolymer in Water Solution: Dynamic and Static Light Scattering and Oscillatory Shear Measurements. *J. Phys. Chem.* **1991**, *95* (4), 1850–1858. <https://doi.org/10.1021/j100157a064>.